Journal of Engineering and Technology for Industrial Applications

ITEGAM-JETIA

Manaus, v.10 n.49, p. 202-211. September/October., 2024.
DOI: https://doi.org/10.5935/jetia.v10i49.1275

ISSN ONLINE: 2447-0228

RESEARCH ARTICLE OPEN ACCESS

ACOUSTICAL NOISE MITIGATION IN SLIP ANGLE CONTROLLED DTC OF OPEN-END WINDING INDUCTION MOTOR DRIVE USING AISPWM BASED TRIPLE RANDOMIZATION SCHEME FOR EV APPLICATION

Ganesh Challa[1] and Dr. M. Damodar Reddy[2]

[1] Resarch Scholar, Dept. of EEE, S. V. University, Tirupati, India.
[2] Professor, Dept. of EEE, S. V. University, Tirupati, India.

[1] http://orcid.org/0000-0001-9683-5763, [2] http://orcid.org/0000-0002-7113-5805

Email: ganesh.challa@gmail.com , mdreddy999@rediffmail.com

ARTICLE INFO

Article History
Received: August 31th, 2024
Revised: October 1th, 2024
Accepted: October 2th, 2024
Published: October 31th, 2024

Keywords:
Acoustical Noise,
AISPWM,
Electric Vehicle,
OEWIM,
RPWM.

ABSTRACT

Industrial and/or Electric Vehicle (EV) drives require low vibration, acoustical noise, as well as efficient utilisation of the DC link. Induction motors with Direct Torque Control (DTC) meet the requirements of EVs and other modern industries. Flux and/or torque oscillations, on the other hand, produce high pitch acoustical noise during steady state, which has an impact on people's health and safety. Hence comprehending and reducing these oscillations are essential for quieter response of EVs. Therefore, EVs and/or workplaces noise reduction has gained significant importance. Space Vector Pulse Width Modulation (SVPWM) enhances the efficiency of DC link utilisation, as required by EVs. However, SVPWM is ineffective at noise reduction. Even if numerous Random PWM (RPWM) approaches minimize f noise, the issue of noise reduction persists due to the lower level of randomization. This study offers an acoustical noise reduction strategy for EV applications, namely Alternate Inverter Switching (AIS) based Hybrid Triple Randomised PWMs (HTRPWM) for DTC of an Open-End Winding Induction Motor Drive with Slip Angle Control. The Harmonic Spread Factor (HSF) is a measure of acoustical noise; the lower the HSF, the less acoustical noise. Thus, the proposed HTRPWMs strive to reduce the HSF and are compared to existing approaches.

I. INTRODUCTION

The worldwide community's enduring dedication to reducing the impacts of global warming leads to the extensive implementation of environmentally friendly technology, such as Electric Vehicle (EV)s and Renewable Energy Sources (RES) [1]-[3]. An EV is a mode of transportation that operates only on electricity. The system has a motor, gearbox, and wheels. The electric motor is the main component of an EV and is responsible for providing the propulsion system. The performance of an EV is greatly impacted by the selection of the electric motor. Induction Motors (IMs) are commonly used in Evs because they are compact, durable, inexpensive, fast, and require minimal maintenance [4]. Evs experience advantages such as improved utilization of the DC bus, less acoustical noise as well as minimized vibrations. The Direct-Torque-Control (DTC) scheme satisfy the rigorous demands of contemporary industry. In recent times, there has been a surge in interest in utilizing DTC for EV applications [5] because to its capability to rapidly adjust torque and minimize the requirement for real-time computations. Nevertheless, it suffers from the drawback of experiencing significant fluctuations in stator current, rotor flux, and torque, as well as having a delayed response due to the presence of hysteresis regulators within the torque and rotor flux control loops [6],[7].

Employing a Multi-Level Inverters (MLI) can effectively mitigate these fluctuations. The Dual Inverter (DI) structure has gained popularity for Open-End Winding Induction Motors (OEWIMs) [8]. It has the potential to be widely used in Evs [9]. The pulse pattern for the switching devices in MLI can be

generated by Pulse Width Modulation (PWM) techniques. Among many PWM techniques, Space Vector Pulse Width Modulation (SVPWM) can mitigate issues arising from disparate switching frequencies. Additionally, it can enhance the efficiency of the DC bus, a crucial factor in satisfying the requirements of Evs. SVPWM-based drives possess inherent constraints such as higher order harmonics, Electro Magnetic Interference (EMI), acoustical noise, and vibrations.

An inherent drawback of SVPWM is vibrations as well as noise emission in industrial drive applications due to higher order harmonics by Voltage Source Inverters (VSIs). This is because there is often a significant overlap between the frequencies at which switches operate and the frequencies that humans are capable of hearing [10],[11]. The inverter's output current comprises of harmonic components at side band frequencies of switching and its multiple. The high order harmonics and narrow bandwidth of these vibrations result in motor vibration and generate irritating noise for the operators. Consequently, the emergence of noise pollution in Evs has raised significant issues regarding efficiency, public well-being, and security. In order to reduce the limited range of noise, it is possible to raise the switching frequency beyond 20 kHz. Nevertheless, it will lead to high switching losses [12], reduces VSI's efficacy, and diminished EV distance of run. The Random PWM (RPWM) method is a highly effective technique for reducing lower band noise by evenly spreading the harmonics in its load current. This is achieved by ensuring a constant rate of switching [13]. The RPWM technique involves random numbers within the control method of the inverter. According to the statistical concept [14], if the switching signal undergoes random fluctuations, the device it regulates amplifies frequency spectra of switching harmonics. The RPWM techniques offer affordable and effective approaches to the above challenges [15].

A number of RPWM algorithms have been suggested by various academicians [16]-[19]. [20] compared the electric and acoustical noise spectrum of SVPWM and two Discontinuous PWM (DPWM) techniques: 30° DPWM and 60° DPWM. This research proved that the first DPWM scheme outperformed the second DPWM scheme in terms of noise reduction. The effects of modern DPWM techniques on motor acoustical noise were investigated by [21]. The study conducted by [22] investigated the application of Direct Sequence spread spectrum technique for grid-tied VSI. [23-25] outlined discrete techniques of RPWM to mitigate harmonic dispersion. Prior studies focused on the distribution of harmonics in VSIs and the amplification of noise spectra in industrial drives. Efforts are currently underway to reduce the noise due to motors used in EV applications [26],[27]. According to [27] showcased the application of a N-State Random Pulse Position Modulation technique to disperse harmonics. Even if numerous RPWM approaches mentioned above minimize acoustical noise, the issue of noise reduction persists due to the lower level (single and dual) of randomization. Hence, present research examines the use of Alternate Inverter Switching (AIS) based Triple Randomized PWM approaches for the mitigation of acoustical noise in Slip Angle Controlled (SAC) DTC of OEWIM drive for EV applications.

II. MATERIALS AND METHODS

II.1 SLIP ANGLE CONTROLLED DTC OF OEWIM DRIVE FED EV

The DTC can be implemented using Slip Speed Control (SSC) [28], or SAC. In the present study SAC based DTC was implemented. Slip angle measured between the stator and rotor flux vectors, and its perfect regulation ensures maximum torque production. SAC is the process of altering the difference between an IM's synchronous and rotor speed, which is crucial for controlling the motor torque. The SAC-based DTC is a sophisticated control method used in electric drive systems, specifically Ims. This technology combines the benefits of both SAC and DTC to provide precise control over motor torque and flux, resulting in improved performance and efficiency.

Figure 1 depicts a block diagram of a SAC based DTC system used in an OEWIM drive for EV applications. A Proportional-Integral (PI) controller is responsible for regulating the error between the reference speed of the EV and its running speed. The regulator generates a required IM torque, which can subsequently compare to actual IM output torque. The PI controller of the torque control loop governs torque deviation and generates the slip angle. This angle then combines with the rotor angle to form a synchronized angle called the stator flux angle. The gains of PI controllers are derived by either a trial-and-error method or an optimized algorithm [30]. The reference stator voltage vectors are obtained from the adaptive motor model. The 2-Φ to 3-Φ conversion is employed to produce 3-Φ sinusoidal reference stator voltage vectors, which can subsequently be modulated by SVPWM and RPWM techniques. Let R_s, L_s = resistance, inductance of the stator,, R_r, L_r = resistance, inductance of the rotor, , L_m = mutual inductance between stator and rotor, p = no. of pole pairs, ψ_s = stator flux linkages, θ_{sl} = slip angle, τ = rotor time constant, I_s = stator current, V_s = stator voltage, ψ_{ds}, ψ_{qs} = d, q axes flux linkages, ψ_{ds}^*, ψ_{qs}^* = commanded d, q axes flux linkages, v_{ds}, v_{qs} = d, q axes stator voltages, v_{ds}^*, v_{qs}^* = commanded d, q axes stator voltages, I_{ds}, I_{qs} = d-axis and q-axis stator currents and v_{a}^*, v_{b}^*, v_{c}^* = commanded 3-Φ stator voltages.

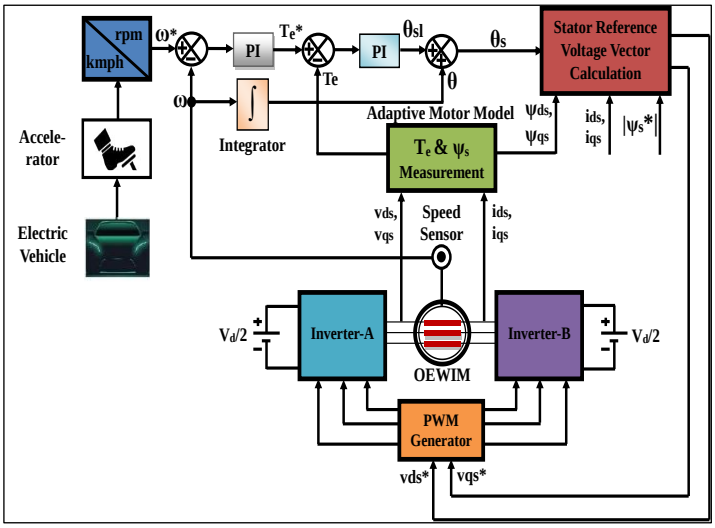

Figure 1: Direct Torque Control of OEWIM fed EV using Slip Angle Control.
Source: Authors, (2024).

The torque produced by an IM is expressed as

$$T_e = \frac{3}{2} p \frac{L_m^2}{R_r L_s^2} \left|\psi_s^2\right| \left(1 - e^{-t/\tau}\right) \left(\frac{d\theta_{sl}}{dt}\right) \quad (1)$$

The torque of the motor can be controlled by adjusting the slip angle during the sample time Δt, while keeping the magnitude of |ψs| constant. The expression for the voltage of the stator in a stationary reference frame can be formulated as

$$\bar{V}_S = \bar{I}_S R_S + \frac{d\bar{\psi}_S}{dt} \quad (2)$$

When voltage drop across stator resistance is ignored, eq. (2) can be expressed as.

$$\Delta\bar{\psi}_S = \bar{V}_S \Delta t \quad (3)$$

The stator flux errors for d and q axes are given by.

$$\Delta\bar{\psi}_{ds} = \bar{\psi}^*_{ds} - \bar{\psi}_{ds} \quad (4)$$

$$\Delta\bar{\psi}_{qs} = \bar{\psi}^*_{qs} - \bar{\psi}_{qs} \quad (5)$$

The commanded stator voltage vectors for d and q axes are given by.

$$V_{ds}^{\ *} = I_{ds} R_S + \frac{\Delta\psi_{ds}}{T_S} \quad (6)$$

$$V_{qs}^{\ *} = I_{qs} R_S + \frac{\Delta\psi_{qs}}{T_S} \quad (7)$$

The d and q axes voltage commanded signals are utilized to produce 3-Φ voltages are expressed by.

$$\begin{bmatrix} V_a^* \\ V_b^* \\ V_c^* \end{bmatrix} = \begin{bmatrix} 0 & 1 \\ -1/2 & -\sqrt{3}/2 \\ -1/2 & +\sqrt{3}/2 \end{bmatrix} \begin{bmatrix} V_{qs}^* \\ V_{ds}^* \end{bmatrix} \quad (8)$$

II.2 PROPOSED MODULATING SIGNAL GENERATION FOR AIS MODE

The 3-Φ sinusoidal commanded voltage signals were written as,

$$v_i = v_m \sin\left(\omega t - 2(x-1)\frac{\pi}{3}\right) \quad (9)$$

where i = a, b, c and x = 1, 2, 3, v_m = peak value of the commanded voltage signal.

The expressions for positive, negative zero sequence voltages can be written as

$$\text{PCM} = \left[(1 - \text{maximum}(va, vb, vc))\right] \quad (10)$$

$$\text{NCM} = \left[(-1 - \text{minimum}(va, vb, vc))\right] \quad (11)$$

Modulated signals for inverter A, B are expressed as

$$v_i^* = \left[1 + (v_i + v_z)\right] * 0.5 \quad (12)$$

$$v_z = k_0 * \text{NCM} + (1 - k_0) * \text{PCM} \quad (13)$$

Here v_z = the zero-sequence voltage, k_o= 0.5 for SVPWM.

Figure 2 depicts the power circuit diagram of the DI structure for producing 3-level output voltage. The AIS-based SVPWM approach requires a single modulated voltage (Vr) and two carrier voltages (Vc_1 and Vc_2) to produce 3-level output voltage as shown in Figure 3.

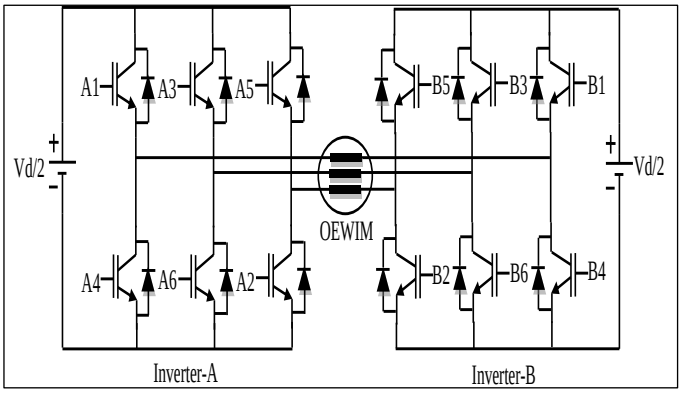

Figure 2: Dual Inverter Structure (3-Level) for OEWIM.
Source: Authors, (2024).

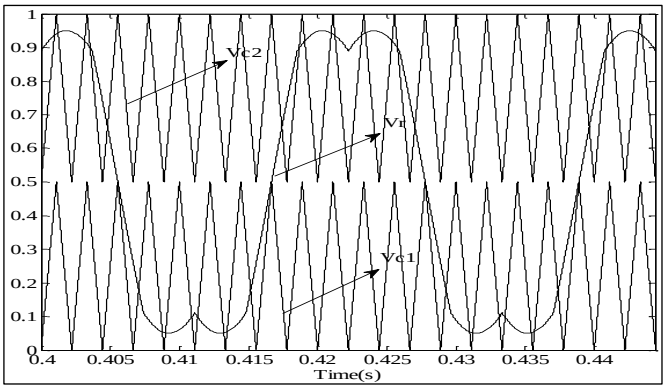

Figure 3: Alternate Inverter Switching Mode for 3-Level DI.
Source: Authors, (2024).

The modulated signal can be compared to the two carrier signals to obtain the gating signals. In the AIS method, Vc1 generates the inverter-A pulse pattern and Vc2 generates the inverter-B pulse pattern. Furthermore, the inverters operate alternately for every 180 degrees, such that while Inverter-A switches, Inverter-B clamps, and vice versa. The stator terminals of the OEWIM receive the effective 3-level output voltage from the two 2-level inverters. VSIs viz. A as well as B are supplied with Vd/2. Table 1 provides a detailed explanation of the conditions required for the DI operation.

Table 1: Switching Logic.

S.No.	Condition	Switch States	
1	Vra > Vc1	A1 Turns ON	A4 Turns OFF
2	Vrb > Vc1	A3 Turns ON	A6 Turns OFF
3	Vrc > Vc1	A5 Turns ON	A2 Turns OFF
4	Vra > Vc2	B1 Turns ON	B4 Turns OFF
5	Vrb > Vc2	B3 Turns ON	B6 Turns OFF
6	Vrc > Vc2	B5 Turns ON	B2 Turns OFF

Source: Authors, (2024).

III. GENERATION OF RANDOM CARRIER

The switched pulse is characterized by three variables: the carrier's switching period (T), the delay-time (δ_m), and the duty-

cycle (d_m.) Out of all the factors, only T and δm are randomized. The delay period δm of an arbitrary pulse with a switching period of T_m can be written as [16].

$$\delta_m = \beta_m (1 - d_m) \quad (14)$$

The carrier's slope βm is randomized within the range of [0, 1], resulting in a random value δm lies within the range of [0, (1 − d_m)]. Due to this, gating signal's position may vary in random at the beginning and finishing position over the fundamental cycle. The triangular carrier is generated by utilizing two variables: T & βm. The Random PWM approaches that were obtained are listed in Table 2.

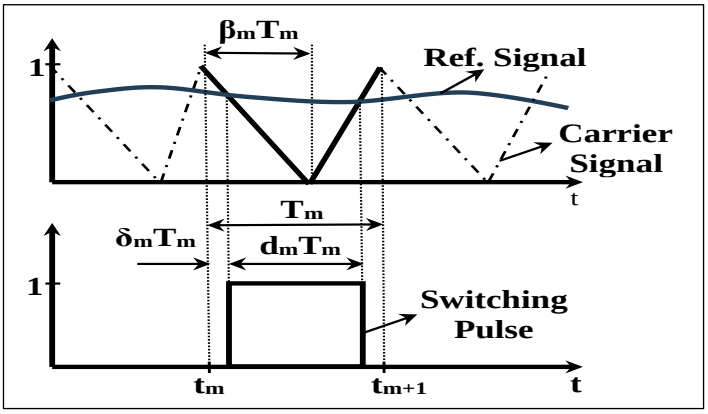

Figure 4: Random Carrier Generation.
Source: Authors, (2024).

Table 2: The βm and T for various PWM Techniques.

S.No.	Modulation Technique	β_m	T
1	SVPWM, RCPWM, RZDPWM	Constant	Constant
2	RPPM	Random	Constant
3	RCFM	Constant	Random
4	RCFM-RPPM	Random	Random

Source: Authors, (2024).

The main difficulty of RPWM approaches is lies in the generation of random numbers. This study utilizes a Pseudo-Random Number Generator (PRNG) that works on the Mersenne Twister (MT) technique. This approach produces quick and good quality uniformly distributed Pseudo-Random Number (PRN)s. The PRNs are real numbers in the closed interval [0,1] and have a long period (2^19937-1). The quantities R_T, R_β define the lower and upper bounds for parameters T, β_m such as (T_{min}, β_{min}) & (T_{max}, β_{max}). The values for δ_m, β_m, and T in table 2 exhibit variance, which can be characterized as follows:

III.1 SPACE VECTOR PULSE WIDTH MODULATION (SVPWM)

In this PWM, the carrier is generated with constant values of β_m and T. Hence switching frequency is fixed and position of the pulse is uniform. Therefore, each triangular carrier having same frequency, equal rise time and fall time as well. In this PWM, randomization is not applied in modulating signal and carrier signal generation.

III.2 RANDOM CARRIER FREQUENCY MODULATION (RCFM)

In this RPWM, the carrier is generated with random T and constant β_m (=0.5). Hence, the switching frequency is randomized and position of the pulse is uniform. Therefore, each triangular carrier having random frequency, equal rise time and fall time. Therefore, pulses are generated with random pulse width. The modulating signal is not randomized in this scheme.

III.3 RANDOM PULSE POSITION MODULATION (RPPM)

In which, the carrier is generated with constant T and β_m is made random for the range of [0,1], the delay time δ_m is random in the range of [0, T] i.e. position of the pulse varies between [0, T]. Hence, each triangular carrier having same frequency, unequal rise time and fall time. Therefore, pulses are generated at non uniform positions within a fundamental sub cycle. The modulating signal is not randomized in this PWM

III.4 RANDOM CARRIER FREQUENCY MODULATION - RANDOM PULSE POSITION MODULATION (RCFM-RPPM)

In this RPWM, both βm and T have randomized values as stated above. Hence, each triangular carrier having random frequency, unequal rise time and fall time. Therefore, pulses are generated with random pulse width and non-uniform positions within a fundamental sub cycle. The modulating signal is not randomized here.

III.5 RANDOM CARRIER PULSE WIDTH MODULATION (RCPWM)

In this case, inverted and non-inverted carriers are selected randomly by generating 0's and 1's. If '0' is generated inverted carrier and/or if '1' is generated non-inverted carrier can be selected. For generating 0 and 1, Pseudo Random Binary Sequence (PRBS) generator can be employed. The modulating signal is not randomized in this PWM.

III.6 RANDOM ZERO VECTOR DISTRIBUTION PULSE WIDTH MODULATION (RZDPWM):

In which, the modulating signal is generated by assigning a value of ko, which is a random number between 0 & 1, in Eq. (13). In this PWM scheme, the duration of the zero vector can be randomized at the beginning and ending edges of the fundamental sub-cycle. This PWM scheme produces a modulating signal called a Random Reference PWM (RRPWM) signal.

III.7 PROPOSED TRIPLE RANDOMIZED PWM SCHEME-1 (RC-RZDPWM-RPPM)

This approach employed randomization for the selection of the carrier, the reference, and the position. It comprises RCPWM, RZDPWM, and RPPM. Here, the RCPWM is achieved through randomly selecting inverted and non-inverted carriers by the generation of 0's and 1's. If '0' is generated inverted carrier and/or if '1' is generated non-inverted carrier can be selected. The Pseudo Random Binary Sequence (PRBS) generator can be used to generate a sequence of 0's and 1's. The RZDPWM is achieved by randomly selecting a value, ko, between 0 & 1, and putting it into equation (13) to determine the modulating signal. The subsequent equations demonstrate the implementation of RPPM.

$$R_\beta = \left[\frac{\beta_{max} - \beta_{min}}{\bar{\beta}} \right] \quad (15)$$

$$\beta \in [\beta_{min}, \beta_{max}] \quad (16)$$

where $\beta min = \bar{\beta}\left(1 - \frac{R_\beta}{2}\right)$ and $\beta max = \bar{\beta}\left(1 + \frac{R_\beta}{2}\right)$ where $\bar{\beta} = 0.5$

The possible values for β_m range from 0 to 1, resulting in a maximum value of R_β equal to 2. The range of R_β is confined to the interval [0,2], hence restricting the range of β_m. For the present study, the value of R_β was fixed at 1.2, which led to a range of β_m values ranging from 0.2 to 0.8. This PWM method generates a carrier signal with a fixed frequency of 3kHz. Based on the 'β_m', the position of the pulse displaced randomly.

The parameter βm varies according to a uniform distribution as under:

$$\beta_m = \beta_{min} + (\beta_{max} - \beta_{min}) * R \quad (17)$$

III.8 PROPOSED TRIPLE RANDOMIZED PWM SCHEME-2 (RC-RZDPWM-RCFM)

This method employed a randomization technique to select the carrier, reference signal, and pulse position. It comprises RCPWM, RZDPWM, and RCFM. The method of implementing RCPWM and RZDPWM was explained in the above section. The following equations illustrate how to implement RCFM.

$$R_T = \left[\frac{T_{max} - T_{min}}{\bar{T}}\right] \quad (18)$$

$$T \in [T_{min}, T_{max}] \quad (19)$$

Where $Tmin = \bar{T}\left(1 - \frac{R_T}{2}\right)$ and $Tmax = \bar{T}\left(1 + \frac{R_T}{2}\right)$,

Here $\bar{T}$ is the mean of switching time T.

The R_T values vary from 0 to 2. Here, R_T was chosen at 0.2 because as T_{max} increases, the presence of lower order harmonics, noise gets more noticeable. This PWM method develops a triangle wave of frequency that can vary between 2727 Hz and 3333.33 Hz, with the normal value of 3000Hz. Here, the gating signal positioned precisely over midpoint of triangular waveform.

The period T varies according to a uniform distribution as under:

$$T = T_{min} + (T_{max} - T_{min}) * R \quad (20)$$

Where 'R' is a random value generated using the MT algorithm, with a value between 0 & 1.

IV. ANALYSIS OF ACOUSTICAL NOISE

Acoustical noise arises from the interaction of multiple frequency components. A study of A-weighting acoustical noise is conducted to determine the overall noise level, taking into account the impact of noise at different frequencies [20]. Unweighted noise is typically expressed in decibel (dB)s, whilst A-weighted noise is expressed in dBAs or dB(A)s. The weighted function $R_A(f)$ is expressed as follows:

$$R_A(f) = \left[\frac{12200^2 f^4}{\left(f^2+20.6^2\right)\left(f^2+12200^2\right)\sqrt{\left(f^2+107.7^2\right)\left(f^2+737.9^2\right)}}\right] \quad (21)$$

f = Frequencies present in noise spectra. The A-weighing noise can be expressed as

$$dBA(f) = dB + 20 * \log\left(R_A(f)\right) \quad (22)$$

Here dB is an unweighted noise derived from the Power Spectral Density (PSD) of the stator current or voltage.

The Harmonic Spreading Factor (HSF) is a key component in acoustic noise assessment as it indicates the extent to which the harmonic spectrum is spread. The objective is to evaluate the PWM method's ability to effectively distribute the harmonic's energy in the harmonic spectrum of a waveform. In general, smaller HSF indicate greater dispersal which means even distribution of harmonic's energy. The formula for HSF [29] can be derived by statistical deviation is as follows

$$HSF = \left[\frac{1}{N}\sum_{i>1}^{N}\left(H_i - H_O\right)^2\right]^{\frac{1}{2}} \quad (23)$$

Here H_i = magnitude of the i^{th} harmonic, H_o = Avg. of magnitudes of the harmonic components $= \frac{1}{N}\sum_{i>1}^{N}\left(H_i\right)$

V. RESULTS AND DISCUSSIONS

Figure 5 shows the simulated results for the modulated signal, phase voltage, stator's currents, electromagnetic torque, motor's speed, and stator's flux trajectory of the SVPWM based DTC of the OEWIM drive using the AIS mode. The results are achieved for the EV operating at a consistent speed of 1200 rpm. Figure 6 displays the spectrum of A-weighting acoustical noise using SVPWM in combination with different RPWM methods. Table 3 displays the HSF for SVPWM and various PWM techniques.

In single randomized RPWM schemes like RCPWM, RPPM, RCFM, and RZDPWM, the degree of randomness is significantly constrained, resulting in a higher HSF compared to other methods. In dual randomised RPWM schemes such as RC-RZDPWM, RC-RPPM, RCFM-RPPM, and RC-RCFM, the degree of randomness is increased slightly and substantially higher compared to single randomised RPWM schemes, resulting in reduced HSF. The traditional triple randomized PWM scheme, such as RC-RCFM-RPPM, shows an increased range of randomness compared to both single-randomized RPWM and dual randomized RPWM schemes, resulting in a reduced HSF.

Table 3: HSF Comparison for Different PWM methods.

S. No.	PWM Method	Randomness	HSF
1	SVPWM [19]	Single	3.74
2	RCPWM [19]	Single	3.57
3	RPPM [17]	Single	2.95
4	RZDPWM [19]	Single	2.89
5	RCFM [16]	Single	2.72
6	RC-RZDPWM [19]	Dual	2.65
7	RC-RPPM [17]	Dual	2.64
8	RCFM-RPPM [16]	Dual	2.28
9	RC-RCFM [19]	Dual	2.12
10	RC-RCFM-RPPM [19]	Triple	1.59
11	RC-RZDPWM-RPPM	Proposed Triple	1.42
12	RC-RZDPWM-RCFM	Proposed Triple	1.28

Source: Authors, (2024).

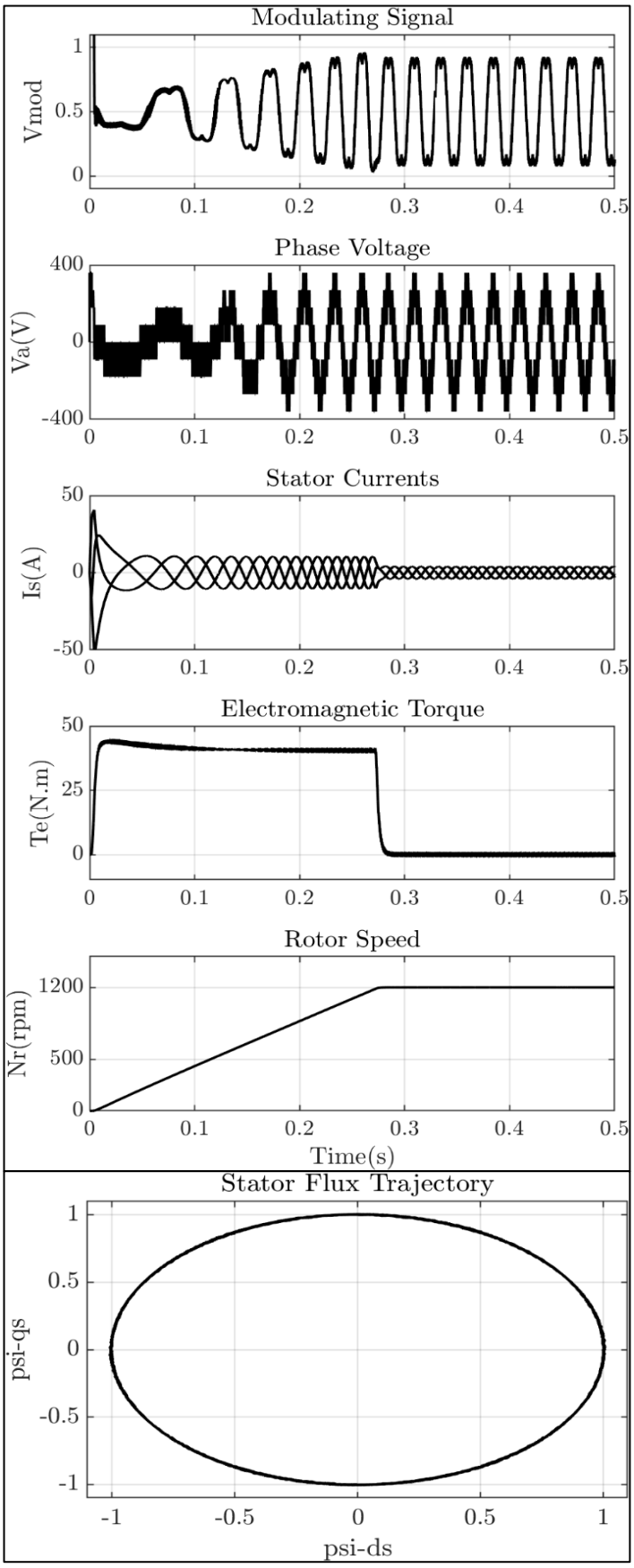

Figure 5: Modulating Signal, Phase Voltage, Stator Currents, Electro Magnetic Torque, Rotor Speed and Stator Flux Trajectory.
Source: Authors, (2024).

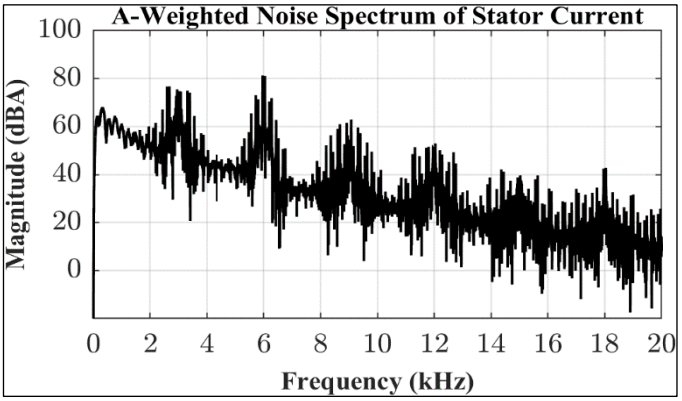

(a) SVPWM

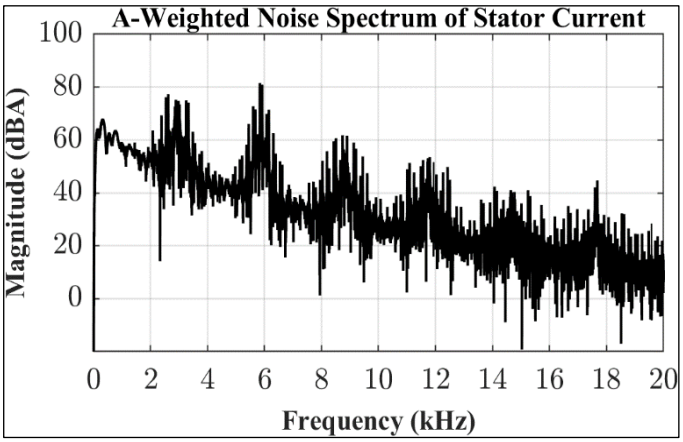

(b) RCPWM

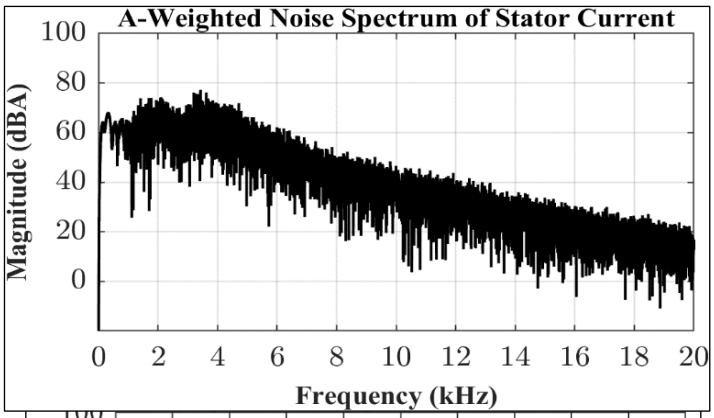

(c) RPPM

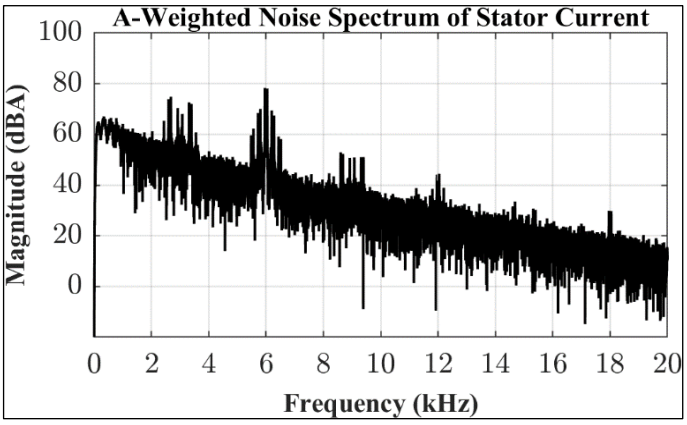

(d) RZDPWM

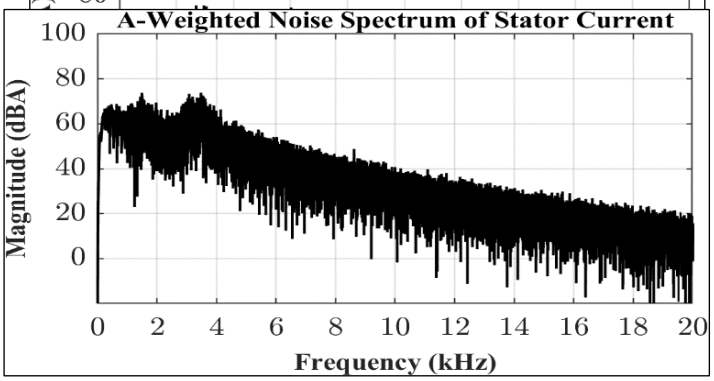

(e) RCFM

(f) RC-RZDPWM

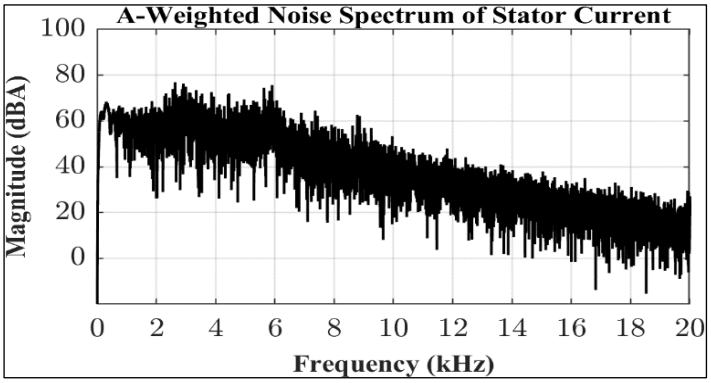

(g) RC-RPPM

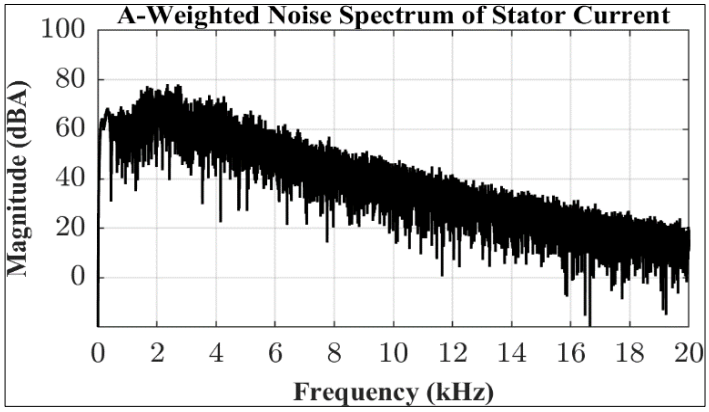

(h) RCFM-RPPM

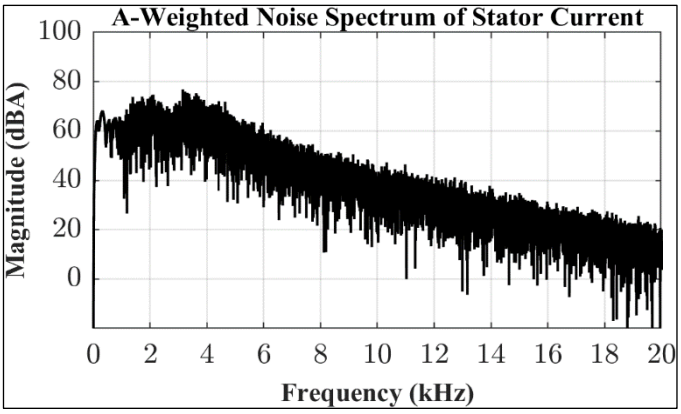

(i) RC-RCFM

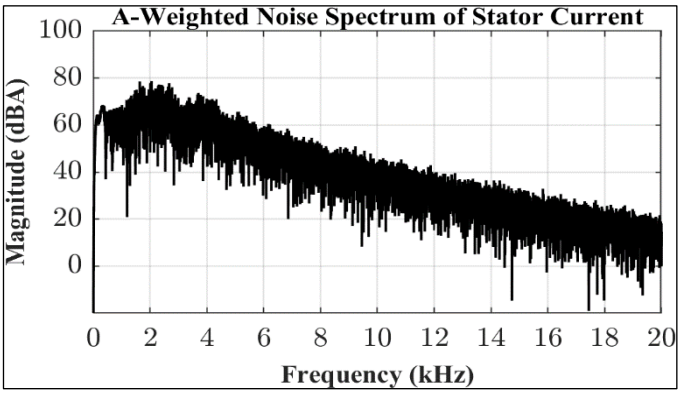

(j) RC-RCFM-RPPM

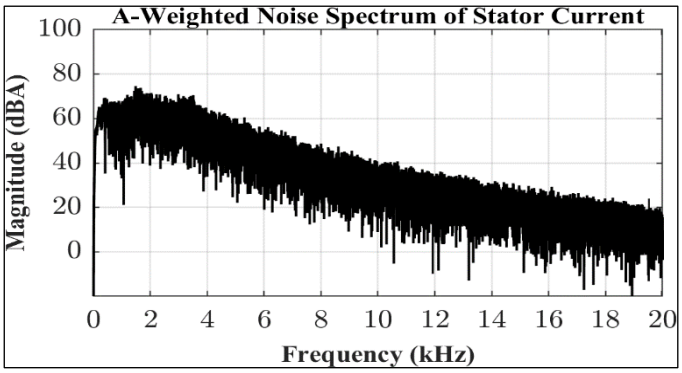

(k) RC-RZDPWM-RPPM

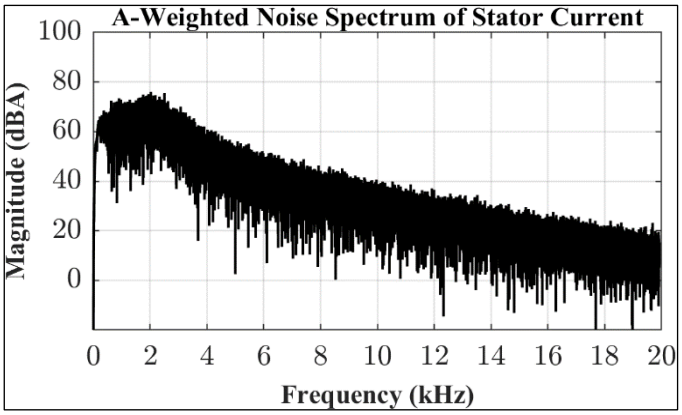

(l) RC-RZDPWM-RCFM.

Figure 6. (a)-(l) A-Weighted Acoustical Noise Spectra for various PWM methods.
Source: Authors, (2024).

The proposed triple randomized PWM schemes, viz. RC-RZDPWM-RPPM and RC-RZDPWM-RCFM, exhibit a significantly higher level of randomness and hence tremondous spread spectrum capabilities when compared to single, dual, and traditional triple randomized PWM schemes as signified by the HSF.

Nonetheless, the RC-RZDPWM-RCFM scheme demonstrates enhanced spread spectrum capability due to the advantageous characteristics of both RZDPWM and RCFM techniques, as evidenced by the HSF value in comparison to RC-RZDPWM-RPPM. The RPWM techniques are effective in minimising EMI. Nonetheless, it experiences challenges related to design and implementation complexity, diminished efficiency, difficulties in filtering, possible stability concerns, and an elevated computational burden.

The ratings of the inverter and induction motor are given as: Vd = 540V, V = 400V, P = 4 kW, p = 4, Nrated = 1470 rpm, f = 50 Hz, Trated = 30 N-m., Rs = 1.57 Ω, Rr = 1.21 Ω, Lm = 0.165 H, Ls = 0.17 H, Lr = 0.17 H and J = 0.089 Kg - m^2.

VI. CONCLUSIONS

This article discusses the implementation of a SAC based DTC strategy for EV applications. It explores the use of the AIS mode and incorporates SVPWM and various RPWM methods. Introducing two new hybrid triple random PWM schemes, namely RC-RZDPWM-RPPM and RC-RZDPWM-RCFM, which are designed to reduce acoustical noise. These methods are then compared with previously described approaches. The suggested techniques exhibit highly efficient for dispersing the harmonic's spectrum, demonstrated by the HSF. This can be attributed to the rise in unpredictability. Therefore, the techniques recommended

have demonstrated remarkable efficacy in reducing acoustical noise, resulting in a 20% reduction in high-frequency noise compared to the conventional triple random PWM method. Compared to RC-RZDPWM-RPPM, RC-RZDPWM-RCFM significantly reduces the noise. In addition, the advancements in Wide Band Gap switches, Uniform Sampling PWM methods, as well as advanced MLIs currently being explored as options to minimise noise in industrial drive applications and EVs.

VII. AUTHOR'S CONTRIBUTION

Conceptualization: Ganesh Challa and Dr. M. Damodar Reddy.
Methodology: Ganesh Challa and Dr. M. Damodar Reddy.
Investigation: Ganesh Challa and Dr. M. Damodar Reddy.
Discussion of results: Ganesh Challa and Dr. M. Damodar Reddy.
Writing – Original Draft: Ganesh Challa.
Writing – Review and Editing: Dr. M. Damodar Reddy.
Supervision: Dr. M. Damodar Reddy.
Approval of the final text: Dr. M. Damodar Reddy.

VIII. REFERENCES

1] H. H. Hussein and A. J. Mahdi, "A Small-scale Inductive Wireless Power Transmission Prototype for Charging Electric Vehicles," 10th International Conference on Smart Grid (icSmartGrid), Istanbul, Turkey, pp. 96-101, Jun. 2022. DOI: 10.1109/icsmartgrid55722.2022.9848722.

[2] F. Zhang, D. C. Kien and H. Takami, "DC-Link Voltage Control Based on Adaptive IRM-ILQ for Stirling Engine Power Supply Vehicle," 12th International Conference on Renewable Energy Research and Applications (ICRERA), Oshawa, ON, Canada, pp. 161-165, August/September 2023, DOI: 10.1109/icrera59003.2023.10269389.
[3] N. V. A. Ravikumar, R. S. S. Nuvvula, P. P. Kumar, N. H. Haroon, U. D. Butkar and A. Siddiqui, "Integration of Electric Vehicles, Renewable Energy Sources, and IoT for Sustainable Transportation and Energy Management: A Comprehensive Review and Future Prospects," 12th International Conference on ICRERA, Oshawa, ON, Canada, pp. 505-511, Aug. /Sept. 2023, DOI: 10.1109/icrera59003.2023.10269421.

[4] S. Pradhan, A. K. Sahoo and R. K. Jena, "Comparison of DTC and SVM - DTC of Induction motor drive for Electric Vehicle application," International Conference on Intelligent Controller and Computing for Smart Power (ICICCSP), Hyderabad, India, pp. 01-06, Jul. 2022, DOI: 10.1109/ICICCSP53532.2022.9862317.

[5] J. Faiz, M. B. B. Sharifian, A. Keyhani and A. B. Proca, "Sensorless direct torque control of induction motors used in electric vehicle," in IEEE Transactions on Energy Conversion, vol. 18, no. 1, pp. 1-10, Mar. 2003, DOI: 10.1109/TEC.2002.805220.

[6] H. Benbouhenni, "Stator current and rotor flux ripples reduction of DTC DFIG drive using FSTSMC algorithm." International Journal of Smart grid, vol.3, no.4, pp. 226-234, Dec. 2019, DOI: 10.20508/ijsmartgrid.v3i4.82.g72.

[7] H. Benbouhenni, "Rotor flux and electromagnetic torque regulation of DFIG using dual PI controllers." International Journal of Smart grid, vol.7, no.4, pp. 227-234, Dec. 2023, DOI: 10.20508/ijsmartgrid.v7i4.308.g311.

[8] H. Stemmler and P. Guggenbach, "Configurations of high-power voltage source inverter drives," Fifth European Conf. on Power Elec. and Appli., Brighton, UK, pp. 7-14, Sept. 1993.

[9] J. Kim, J. Jung and K. Nam, "Dual-inverter control strategy for high-speed operation of EV induction motors," in IEEE Transactions on Industrial Electronics, vol. 51, no. 2, pp. 312-320, Apr. 2004, DOI: 10.1109/TIE.2004.825232.

[10] Y. Huang, Y. Xu, W. Zhang and J. Zou, "Hybrid RPWM Technique Based on Modified SVPWM to Reduce the PWM Acoustic Noise," in IEEE Transactions on Power Electronics, vol. 34, no. 6, pp. 5667-5674, Jun. 2019, DOI: 10.1109/TPEL.2018.2869980.

[11] Y. Lv, S. Cheng, Z. Ji, X. Li, D. Wang, Y. Wei, X. Wang, and W. Liu, "Spatial-Harmonic Modeling and Analysis of High-Frequency Electromagnetic Vibrations of Multiphase Surface Permanent-Magnet Motors," in IEEE Transactions on Industrial Electronics, vol. 70, no. 12, pp. 11865-11875, Dec. 2023, DOI: 10.1109/TIE.2023.3239905.

[12] J. Y. Chai, Y. H. Ho, Y. C. Chang and C. M. Liaw, "On Acoustic-Noise-Reduction Control Using Random Switching Technique for Switch-Mode Rectifiers in PMSM Drive," in IEEE Transactions on Industrial Electronics, vol. 55, no. 3, pp. 1295-1309, Mar. 2008, DOI: 10.1109/TIE.2007.909759.

[13] M. M. Bech, J. K. Pedersen and F. Blaabjerg, "Field-oriented control of an induction motor using random pulsewidth modulation," in IEEE Transactions on Industry Applications, vol. 37, no. 6, pp. 1777-1785, Nov.-Dec. 2001, DOI: 10.1109/APEC.2000.822615.

[14] A. M. Stankovic, G. E. Verghese and D. J. Perreault, "Analysis and synthesis of randomized modulation schemes for power converters," in IEEE Transactions on Power Electronics, vol. 10, no. 6, pp. 680-693, November 1995, DOI: 10.1109/63.471288.

[15] X. Zhu et al., "A Passive Variable Switching Frequency SPWM Concept and Analysis for DCAC Converter," in IEEE Transactions on Power Electronics, vol. 37, no. 5, pp. 5524-5534, May 2022, DOI: 10.1109/TPEL.2021.3123190.

[16] A. Boudouda, N. Boudjerda, and A. Aibeche, "dSPACE-based dual randomized pulse width modulation for acoustic noise mitigation in induction motor." Journal of the Brazilian Society of Mechanical Sciences and Engineering (Spinger), vol. 44, no. 10, Sept. 2022, DOI: 10.1007/s40430-022-03814-2.

[17] J. Xu, Z. Nie and J. Zhu, "Characterization and Selection of Probability Statistical Parameters in Random Slope PWM Based on Uniform Distribution," in IEEE Transactions on Power Electronics, vol. 36, no. 1, pp. 1184-1192, Jan. 2021, DOI: 10.1109/TPEL.2020.3004725.

[18] P. Madasamy, R. Verma, C. Bharatiraja, J. Barnabas Paul Glady, T. Srihari, J. L. Munda, L. Mihet-Popa, "Hybrid Multicarrier Random Space Vector PWM for the Mitigation of Acoustic Noise," Electronics, vol. 10, no. 12, pp. 1-19, Jun. 2021, DOI: 10.3390/electronics10121483.

[19] S. Nithya Lavanya, T. Bramhananda Reddy, and M. Vijaya Kumar, "Constant and variable switching frequency random PWM strategies for open-end winding induction motor drive". J. Power Electron., vol. 20, pp. 1488–1495, Sept. 2020, DOI: 10.1007/s43236-020-00137-0.

[20] A. C. Binoj Kumar, B. Saritha and G. Narayanan, "Experimental Comparison of Conventional and Bus-Clamping PWM Methods Based on Electrical and Acoustic Noise Spectra of Induction Motor Drives," in IEEE Transactions on Industry Applications, vol. 52, no. 5, pp. 4061-4073, Sept. - Oct. 2016, DOI: 10.1109/TIA.2016.2584578.

[21] A. C. Binoj Kumar, J. S. S. Prasad, and G. Narayanan, "Experimental Investigation on the Effect of Advanced Bus-Clamping Pulse Width Modulation on Motor Acoustic Noise." IEEE Trans. on Ind. Elec., vol. 60, no. 2, pp. 433-439, Feb. 2013, DOI: 10.1109/tie.2012.2190371.

[22] R. Alavanthan and A. Kavitha, "Digital implementation of DS-SFH hybrid spread-spectrum modulation technique in three-phase voltage-source converter." Electrical Engineering (Spinger), vol. 104, no. 3, pp. 1413-1423, Oct. 2021, DOI: 10.1007/s00202-021-01388-1.

[23] Y. Wang, J. Liu, B. Lu and M. Wang, "A Novel Discrete Hybrid Dual Random SVPWM Scheme for Reducing PMSM Harmonic Intensity," in IEEE/ASME Transactions on Mechatronics, vol. 28, no. 3, pp. 1425-1435, Jun. 2023, DOI: 10.1109/TMECH.2022.3220519.

[24] S. Bhattacharya, D. Mascarella, G. Joos and G. Moschopoulos, "A discrete random PWM technique for acoustic noise reduction in electric traction drives," IEEE Energy Conversion Congress and Exposition (ECCE), Montreal, QC, Canada, pp. 6811-6817, Sept. 2015, DOI: 10.1109/ECCE.2015.7310613.

[25] A. R. González, J. R. H. Larrubia, F. M. P. Hidalgo, M. J. M. Gutiérrez, "Discontinuous PWM Strategy with Frequency Modulation for Vibration Reduction in Asynchronous Machines" Machines, vol. 11, no. 7, pp. 1-22, May 2023, DOI: 10.3390/machines11070705.

[26] R. K. Thakur, R. M. Pindoriya, R. Kumar, and B. S. Rajpurohit, Transportation Electrifi cation, India: Wiley, 2022, ch.5, DOI: 10.1002/9781119812357.ch5.

[27] P. Zhang, S. Wang and Y. Li, " Three-Phase Two-Level VSIs With Significant PWM Harmonics Dispersion and Improved Performance Using Generalized N-State Random Pulse Position SVPWM With Constant Sampling Frequency" in

IEEE Transactions on Power Electronics, vol.39, no.1, pp.1394-1409, Jan. 2024, DOI: 10.1109/TPEL.2023.3328213.

[28] S. Sarada, N. Ravisankara Reddy,"Comparative Switching and Conduction Loss Analysis of a SVPWM and DPWM based DTC of Open-End Winding Induction Motor Drive", International Journal of Renewable Energy Research, vol.12, no.4, pp.1954-1965, Dec. 2022, DOI: 10.20508/ijrer.v12i4.13466.g8618.

[29] K. -S. Kim, Y. -G. Jung and Y. -C. Lim, "Shaping the spectra of the acoustic noise emitted by three-phase inverter drives based on the new Hybrid Random PWM technique," 37th IEEE Power Electronics Specialists Conference, Jeju, Korea (South), pp. 1-6, Jun. 2006, DOI: 10.1109/pesc.2006.1711823.

[30] Venkata Anjani Kumar G, Damodar Reddy M, "Optimized PI tuning of DG-integrated shunt active power filter using biogeography-based optimization algorithm" Journal Européen des Systèmes Automatisés, vol. 56, no. 6, pp. 907-916, Dec. 2023, DOI: 10.18280/jesa.560602.